

Preparation, characterization, and monitoring of an aqueous graphite ink for use in binder jetting

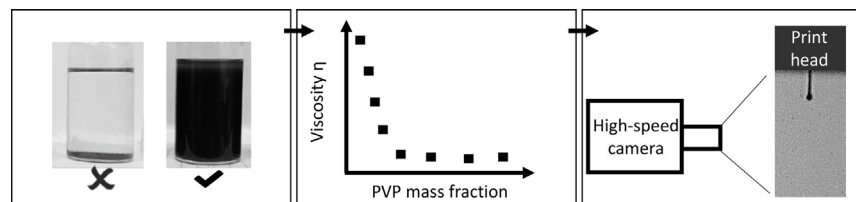
Maja Lehmann*, Cara G. Kolb, Flavia Klinger, Michael F. Zaeh

Institute for Machine Tools and Industrial Management, Department of Mechanical Engineering, Technical University of Munich, Boltzmannstr. 15, 85748 Garching, Germany

HIGHLIGHTS

- Polyvinylpyrrolidone is usable as a binder and simultaneously as a dispersant.
- Formation and velocity of the drops are influenced by the particle mass fraction.
- Increasing the particle load can lead to a deterioration of the printing behavior.
- Inks with a particle load up to 5 m% show a drop formation without satellite drops.

GRAPHICAL ABSTRACT



ARTICLE INFO

Article history:

Received 4 May 2021

Accepted 1 June 2021

Available online 04 June 2021

Keywords:

Binder jetting
Particle loaded ink
Drop monitoring
Printability

ABSTRACT

The use of particle loaded inks in binder jetting offers several advantages, such as the improved sintering ability or the adaption of material properties in a printed part. Various aspects have to be considered for the preparation and the printability. A high stability is necessary, therefore agglomeration and sedimentation of the particles must be avoided. It is also important that long filaments and thus satellite droplets are not formed during printing. In this study, inks loaded with graphite nanoparticles were investigated regarding their stability and drop formation behavior to qualify them for reliable processing in binder jetting. Polyvinylpyrrolidone (PVP) was used as a binder for the binder jetting process and simultaneously as a dispersing agent for the nanoparticles. The PVP mass fraction was investigated for its dispersion effect. To meet the print head requirements, the particle size distribution had to be below 1 μm . To destroy agglomerates with a diameter above this limit, ultrasonic treatment was used. The duration of the ultrasonic treatment was examined to identify the minimum time required to obtain a well dispersed ink. Particle loaded inks were then prepared and the fluid mechanical properties were determined for inks with different particle mass fractions. Monitoring of the drop formation provided information about a stable drop generation, the filament lengths, and the velocity of the drops. It was possible to qualify inks with a maximum particle mass fraction of 10 m% for the binder jetting process.

© 2021 The Authors. Published by Elsevier Ltd. This is an open access article under the CC BY-NC-ND license (<http://creativecommons.org/licenses/by-nc-nd/4.0/>).

1. Introduction

Binder jetting is a powder-based additive manufacturing technology that uses an ink to solidify the single layers of the powder

bed. The bonding of the powder allows the layer-by-layer manufacturing of a stable green part. Adding nanoparticles to this ink can improve the part quality, as the particles serve as sintering additives or increase the packing density. Bai et al. [1] added silver nanoparticles to the ink and solidified silver microparticles in the powder bed. Due to a lower melting temperature of the nanoparticles, their consolidation resulted in a higher bonding strength during the heating process. This effect led to a higher green part

* Corresponding author.

E-mail addresses: Maja.Lehmann@iwb.tum.de (M. Lehmann), Cara.Kolb@iwb.tum.de (C.G. Kolb).

strength, improved the dimensional accuracy, and increased the ductility of the silver parts.

Additionally, nanoparticles offer the possibility of selectively changing the material composition in the part. Godlinski and Morvan [6] produced graded green parts by applying a functional ink loaded with carbon black nanoparticles to a steel powder bed. These nanoparticles acted as alloying elements and changed the local strength and hardness properties.

However, Tsai et al. [22] showed that nanoparticles affect the fluid mechanical properties, the drop formation, and the stability of an ink. To understand their relationship, they are explained in detail.

1.1. Stable drop formation

A stable drop formation is necessary to ensure the positional accuracy and a reproducible printing resolution. Jang et al. [7] postulated that inadequate drop formation is characterized primarily by the formation of long filaments, which results in satellite drops and influences the precision of the drop placement negatively.

For the drop formation in a piezoelectric print head, the viscosity, the density, and the surface tension of the liquid are decisive. Fromm [5] summarized these ink properties in the dimensionless Ohnesorge number Oh .

$$Oh = \frac{\sqrt{We}}{Re} = \frac{\eta}{\sqrt{\rho\gamma L}} = Z^{-1} \quad (1)$$

We is the Weber number, Re the Reynolds number, η the viscosity, ρ the density, γ the surface tension, and L the characteristic length of the drop formation process. Polsakiewicz and Kollenberg [16] stated that the nozzle diameter of the print head is usually used for this length.

With the help of the inverse Z of the Ohnesorge number, a stable drop formation and thus a good printability of an ink can be predicted. In the literature there are different approaches for the classification of Z :

- Reis and Derby [17] found that for drop-on-demand systems such as piezoelectric print heads an ink should have a Z value between 1 and 10. Lower values of Z led to viscous dissipation and thus no drops were formed and values higher than 10 resulted in the formation of long filaments, which caused satellite drops.
- Jang et al. [7] redefined the range of the values for Z for good printability. Inks with a Z value under 4 already showed long-lived filaments during the drop formation. When Z exceeded the value 14, the ink was not able to form a single drop during printing due to low viscosity.
- Zhong et al. [25] further narrowed down the range for Z . They numerically determined a Z value between 4 and 8.

The viscosity, the surface tension, and the density of an ink determine Z and are thus limited by these defined ranges. The viscosity and the surface tension are particularly influenced by particles. An increasing particle volume fraction increases the viscosity and can even lead to a change in the fluid mechanical behavior, as Mueller et al. [12] described.

1.2. Stability of a particle loaded ink

In addition to the drop formation, the stability of an ink is important for good printability. Unstable inks tend to sediment and agglomerate, which affects the printing behavior and leads to clogging of the print head nozzles. According to Utela et al. [24], the initial particle size, the size of the agglomerates, and the

viscosity influence the stability of an ink. Mewis [11] analyzed the influence of the Brownian forces on the sedimentation behavior of particles. Small particles are prevented from sinking by these forces. If the particles form agglomerates, Brownian motion no longer occurs and the particles sediment. Nanoparticles tend to agglomerate easily due to their high surface area, and a dispersant is required to uniformly distribute the particles throughout the ink. Since agglomeration and sedimentation cannot always be prevented, the particle size distribution is an indicator of whether clogging of the nozzles may occur. The most suitable type of print heads has a nozzle diameter around 50 μm . Utela et al. [24] stated that the agglomerates of the particles need to be at least 50 times smaller to prevent clogging or bridging of the nozzle. The higher the viscosity is, the slower is the sedimentation. However, high viscosity values influence the printing behavior. Consequently, Z conflicts with the stability as the viscosity increases.

1.3. Approach

This study focuses on the preparation of a stable, printable ink loaded with graphite nanoparticles. The ink was designed for use in binder jetting to produce tungsten carbide parts with local gradients, as published in the concept of Lehmann and Zaeh [9]. Depending on the desired gradient, different particle fractions should be dispersed in the ink. Therefore, inks with varying particle mass fractions were prepared and characterized. Zhu et al. [26] showed that a non-ionic dispersant such as polyvinylpyrrolidone (PVP) is suitable for improving the stability of graphite nanoparticles in water. The preparation route was determined and the influence of the PVP mass fraction and the duration of the ultrasonic treatment was investigated due to their dispersion effect. Using the finding outlined by Utela et al. [24], the required value for the maximum particle size was set to 1 μm . The viscosity, the density, and the surface tension of the ink had to meet the requirements of the print head and had to result in the correct balance of inertial, viscous, and surface tension forces during the drop formation. The calculated Ohnesorge number described this balance and the inverse Z gave the theoretical printability of the inks. The validation of the printability and the characterization of the drops were conducted by in-process drop monitoring.

2. Experimental

The description of the experimental procedure of this study is divided into three subsections. These subsections summarize the preparation process and the characterization of the different experiments. An overview of the objectives and their relevance is given in Table 2.

2.1. Preparation of the particle loaded ink

Using the procedure laid out in Polsakiewicz [15], a water-based ink with Newtonian fluid behavior was used as the base ink for the experiments. To adapt the base ink to the print head, the viscosity was adjusted by varying the mass fraction of ethylene

Table 1
Composition of the base inks in m% (based on [15]) with the variations of the ethylene glycol and the water content

Ink	Water in m%	Ethylene glycol in m%	Isopropanol in m%	PVP in m%
A	55.87	22.39	8.7	13.04
B	45.87	32.39	8.7	13.04
C	35.87	42.39	8.7	13.04
D	28.74	47.10	8.7	13.04

Table 2
Preparation route and characterization of the different partial objectives and their relevance for reliable printing

Objectives	Components	Preparation process	Characterization/Relevance
Base ink	Water, PVP, isopropanol, ethylene glycol (EG)	Adjustment of the EG content, mixing the components, magnetic stirring for 30 min	Drop monitoring / base ink for the particle loaded inks
Particle size distribution	Base ink, particle type A and B, mass fraction of 10%	Mixing of the components, magnetic stirring for 30 min, sonication (160 s)	Laser diffraction analyzer / right arrow prevent clogging of the printhead
PVP mass fraction	Water, PVP (1 to 800 m%) referred to solid content, 10 m% particles (type A)	Mixing water with PVP, magnetic stirring for 30 min, adding 10 m% of particles, magnetic stirring for 30 min, sonication (160 s)	Viscosity measurement / dispersion of the particles
Duration of the ultrasonic treatment	Base ink, 10 m% particles (type A)	Mixing of the components, magnetic stirring for 30 min, variation of the duration of the sonication between 80 and 280 s	Laser diffraction analyzer / homogenization
Particle loaded inks	Base ink, 1, 5, 10, and 15 m% particles (type A)	Mixing of the components, magnetic stirring for 30 min, US homogenization (160 s)	Fluidmechanical properties, drop monitoring / printability

glycol and water. The compositions of the prepared base inks are shown in Table 1.

PVP (Luvitec 17, BASF, Germany) was used as a binder for the subsequent binder jetting process and simultaneously as a dispersant for the nanoparticles in the ink. Isopropanol defined the surface tension of the base ink. PVP was dissolved in the water-isopropanol-ethylene-glycol mixture for 30 min using a magnetic stirrer.

For the preparation of the particle loaded inks, graphite nanoparticles (Graphite (C) Nanopowder, Nanografi, Turkey) with a mean diameter of less than 50 nm (referred to as type A) in the range of 1 to 15 m% were added to the base ink. The mixture was stirred for another 30 min.

To compare different sizes of particles, an ink with graphite nanoparticles (ACS Material, USA) with a diameter of 400 to 600 nm (referred to as type B) and 10 m% was prepared.

In order to capture the influence of the PVP mass fraction, inks with a constant particle mass fraction of 10% were prepared with water, PVP, and particles.

For the homogenization, the particle loaded inks were sonicated for 160 s with a 1 min cooling break after each 20 s. To determine the influence of the duration of the ultrasonic treatment, the inks were sonicated in a time interval of 80 s to 280 s.

2.2. Characterization

The rheological properties of the inks were measured using a rotational rheometer (Kinexus lab +, Netzsch, Germany) with a 40 mm plate-plate geometry and a sample gap of 0.1 mm. The viscosity was measured at a shear rate of 80 s⁻¹ for 3 min, capturing 36 single point measurements to compare the influence of the PVP mass fraction and to determine the viscosity of the inks with different particle fractions. Samples were kept at 25°C at all times. The particle size distribution was determined using a laser diffraction analyzer (SALD-2201, Shimadzu, Japan). For the dilution of the inks, deionized water was used as the medium with a ratio of 1:500. The density of the inks was calculated theoretically. The surface tension of the inks was examined by the stalagmometric method developed by [21]. Deionized water was used for the calibration. For each measurement, 20 drops were weighed and three measurements per ink were performed.

2.3. Drop monitoring

A test rig was set up for the drop monitoring (see Fig. 1). The drops were generated by a piezoelectric print head (Spectra SL-128 AA, Fujifilm, Japan) with a nozzle diameter of 50 μm in a binder jetting printer (VTS128, Voxeljet Technology GmbH, Germany). The voltage was set to 80 V and a pulse duration of 7 μs was used. A stable drop formation was achieved for the base ink at a frequency

of 1000 Hz. Printing of the particle loaded inks with 10 m% was not possible at this frequency, thus it was reduced to 250 Hz for all inks to ensure comparability. To record the drops and analyze the drop formation, a high-speed camera (iSpeed, Olympus, Japan) with a Sigma objective lens with 105 mm focal length and 68 mm extension rings was used. The high-power LED (M405LP1, Thorlabs, Inc., USA) was focused with a collimator (SM2P50-A, Thorlabs, Inc., USA) and controlled by an LED driver (LEDD1B T-Cube, Thorlabs, Inc., USA).

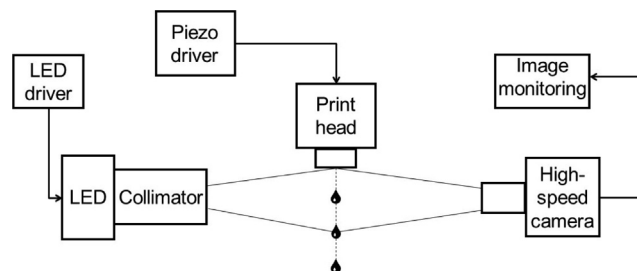


Fig. 1. Schematic image of the monitoring setup

Each ink was recorded during two runs at the printer, and several videos were recorded of each run. To capture images of the drop formation, a high image quality was necessary. Therefore, a frame rate with 2000 frames per second (fps) was employed. To measure the velocity of the drops, a higher frame rate was needed. Thus, it was adjusted to 100000 fps. A summary of this data is shown in Table 3.

The velocity was calculated from the number of pixels and the frame rate. The distance of the drops to the nozzle (number of pixels) was determined as a function of time (frame rate).

Table 3
The frame rate and the image quality for the monitoring images and the velocity calculation

Objective	Frame rate in fps	Image quality in pixels
Drop formation	2000	2048 × 512
Velocity	100,000	96 × 72

3. Results and discussion

3.1. Particle size distribution

To ensure that the print head nozzles do not become clog-ged with agglomerates, the particle size distribution of the particles

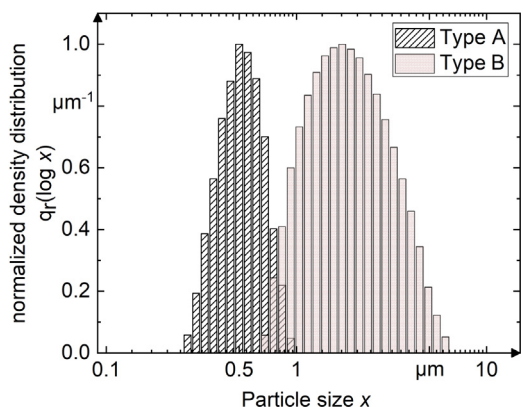


Fig. 2. Comparison of the particle size distribution of nanoparticles with an initial size of 600 nm (type B) and 50 nm (type A) in an aqueous solvent containing 10 m% of particles

of types A and B was investigated. Fig. 2 displays the normalized density distribution over the particle size of these two types of nanoparticles.

Both types of nanoparticles show agglomerated particles. The agglomerates of the type A remain under the defined threshold of 1 μm . The major part of these particles has a size in a three-digit nanometer range. The particles of type B also form agglomerates. Due to the greater initial size, their size is above the defined limit. The maximum particle size reaches 6 μm . Due to their different diameters, the particle size distribution of both types lies in a range above the initial size of the particles. Comparing the agglomeration rate, type B showed a more effective dispersion behavior, but quickly exceeded the defined threshold value. The particles of type A had a higher surface area, which usually leads, according to Nanda et al. [14], to an increased tendency to agglomeration due to their higher surface energy. Zhu et al. [26] postulated that the stabilization effect of a non-ionic dispersant is based on its concentration on the surface of the particles. Ueki et al. [23] stated that the dispersant forms a molecular layer that causes a repulsive force between the dispersant layers of the other particles and reduces the particle–particle interactions. Thus, for smaller particles, more PVP can be adsorbed at the surface, and too low fractions of the dispersant result in an insufficient dispersion of the particles. However, the particle size remained below the limit, and the particles were used for binder jetting processing. Since an unsuitable concentration of the dispersant in an ink affects the dispersion effect negatively, the influence of the PVP mass fraction was investigated for the particles of type A.

3.2. Influence of the PVP mass fraction on the dispersion of the particles

The influence of the PVP mass fraction on the viscosity, and thus on the stability of the ink, is shown in Fig. 3. The PVP mass fraction refers to the solid mass content and the standard deviation results from 36 single point measurements.

For small quantities of PVP the viscosity of the ink has a value between 0.08 and 0.15 Pas and shows a high standard deviation. According to Mewis [11], this indicates the presence of agglomerates in the ink. With increasing PVP mass fraction, the viscosity decreases to a minimum of 0.0013 Pas at 20 m% PVP and the standard deviation is reduced. Up to a PVP mass fraction of 100%, the viscosity remained constant. In the experiment, the flowability of the ink was improved by the reduction of the particle–particle interactions due to a high dispersion of the nanoparticles. This

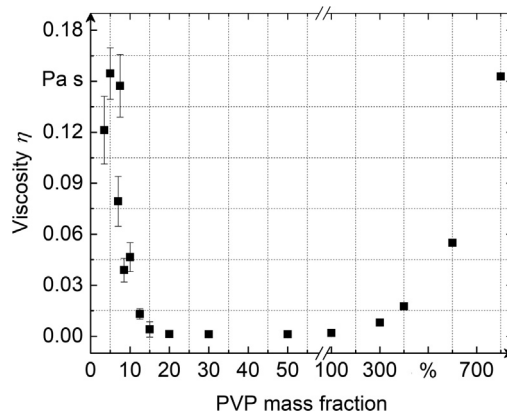


Fig. 3. Viscosity of an ink with a particle load of 10 m% at a shear rate of 80 s^{-1} over the PVP mass fraction

effect was already observed by Schröckert et al. [19]. When the PVP mass fraction was further increased, the viscosity rose again. The surface of the particles was then completely coated by PVP and the remaining PVP molecules in the ink increased the viscosity.

The base ink had a PVP mass fraction of 13.04%. Referring this fraction to the solid mass content, theoretically a particle mass fraction of 65.2% can be dispersed in the base ink.

3.3. Influence of the duration of the ultrasonic treatment

To evaluate the influence of the duration of the ultrasonic treatment, the particle size distribution was measured after different time intervals and the d_{50} value is plotted versus the duration of the ultrasonic treatment in Fig. 4.

Three measurements were recorded for each duration. The standard deviation was too small to be displayed in the diagram and was in the range of a few nanometers.

The d_{50} value decreased with an increasing duration of the ultrasonic treatment. At 160 s the suspension was well dispersed and equivalent to the results of the particle size distribution in Fig. 2. A longer ultrasonic homogenization did not improve the dispersing of the particles, neither was a reagglomeration of the particles caused. However, the relationship from Fig. 4 demonstrates that ultrasonic treatment is necessary. Consequently, for the preparation of the particle loaded ink for the printing process, all samples were sonicated for 160 s.

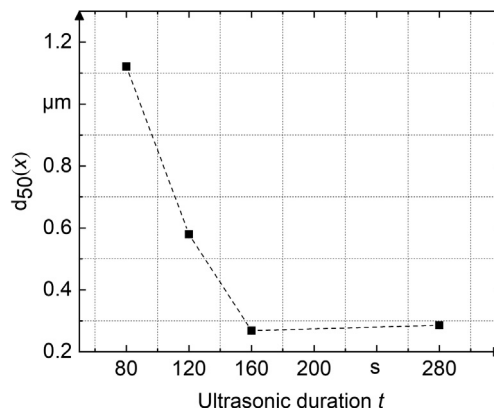


Fig. 4. d_{50} value of the particle size distribution over the duration of the ultrasonic treatment

3.4. Printability

According to Derby and Reis [3], the range $1 < Z < 10$ is defined as the printable region (white region in Fig. 5). The lines *a* and *b* added by Derby [2] limit the printable area, since below *a* the energy is not sufficient for drop formation and when the velocity of a drop exceeds the line *b*, splashing occurs.

Analogous to Derby and Reis [3], in Fig. 5 *We* is plotted against *Re*. The *Z* values of the inks A, B, C, and D were calculated and are classified within the printable range. Drop monitoring images of the printed inks sorted according to their *Z* value are added to the graph to visualize the printing behavior.

With increasing ethylene glycol content, the viscosity rose and *Z* decreased. All inks had a *Z* value in the range defined by Derby and Reis [3]. For the print head used, the inks A (*Z* = 8.92) and B (*Z* = 6.84) were printable, but formed satellite drops. The ink D with the *Z* value of 3.55 was too viscous to be printed. A stable drop formation was achieved with ink C with a *Z* value of 5.15. This ink was used as the base ink for the preparation of the particle loaded inks. The results show that the range of the *Z* values defined by Zhong et al. [25] best delimits the printable region of the prepared inks. For stable spherical drops, the upper limit of *Z* was reduced to 6 in this work. To identify the printability of the particle loaded inks, the fluid mechanical properties viscosity, density, and surface tension were used to determine the Ohnesorge number and *Z* for each ink. The results are presented in Table 4. With increasing particle fraction the viscosity and the density of the inks increased. This goes in line with findings from the literature, such as the research of Rutgers [18]. For 1 m% and 5 m% the surface tension decreased, while it slightly increased for 10 m% and 15 m%. This can also be explained by the high viscosity and thus the higher probability of measurement errors with the stalagmometric method. There are different findings in the literature regarding the influence of the particle fraction on the surface tension. Tanvir and Qiao [20] showed that the surface tension of a suspension increases with increasing particle fraction due to molecular forces, such as the Van der Waals forces. In contrast, Murshed et al. [13] observed a reduction of the surface tension with an increasing particle fraction. They explained this effect, among other things, by the Brownian motion. Dong and Johnson [4] showed that at low particle volume fraction the internal energy is reduced by a spontaneous adsorption of the particles at the surface, leading to a decrease of

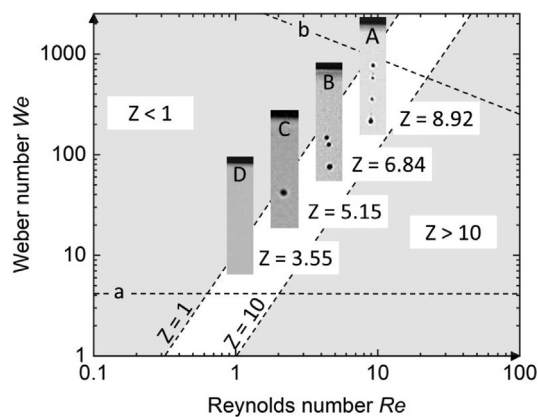


Fig. 5. The *We* number is plotted against the *Re* number as done by Derby and Reis [3] with a classification of the different inks by their *Z* number in the white, printable range. The left limit of the printable region represents a *Z* value of 1, the right limit a *Z* value of 10. The drop monitoring images in the bars are used to visualize the drop formation behavior. In the area below the line *a* there is not enough energy for the drop formation. Line *b* indicates the onset of splashing.

Table 4

Values of the fluid mechanical properties and calculated Ohnesorge number of the particle loaded inks with different particle fractions

Fraction	η	ρ	γ	<i>L</i>	<i>Oh</i>	<i>Z</i>
in m%	in mPas	in kg/m ³	in mN/m	in m	-	-
0	8.98	1.041·10 ³	41.11	5·10 ⁻⁵	0.194	5.15
1	8.89	1.047·10 ³	38.37	5·10 ⁻⁵	0.198	5.04
5	10.49	1.066·10 ³	37.19	5·10 ⁻⁵	0.236	4.24
10	14.44	1.089·10 ³	40.35	5·10 ⁻⁵	0.308	3.25
15	16.96	1.111·10 ³	40.38	5·10 ⁻⁵	0.358	2.79

the surface energy of the suspension. As the particle volume fraction increased, the capillary attraction between the particles led to an increase in surface tension.

However, in this study we observed that the surface tension and the density affect *Z*, but increasing the particle mass fraction has the largest impact on the viscosity and thus the greatest influence on *Z*. The measurement errors in the surface tension can therefore be neglected.

Theoretically, the inks with a mass fraction of particles up to 15% should be printable due to their *Z* value. However, the experiments showed that it was not possible to print the 10 m% and 15 m% at a frequency of 1000 Hz. Jang et al. [7] evaluated the influence of *Z* on the frequency. The lower the *Z* value is, the longer the drop formation takes. The time of the drop formation can be equated with the maximum allowable frequency. Thus, the frequency was set to the lowest possible value of 250 Hz. With this frequency the inks up to a mass fraction of 10% were printed. Even at 250 Hz the drop formation of the ink with a mass fraction of 15% was not possible.

3.5. Drop monitoring

3.5.1. Drop formation

The drop formation was investigated by drop monitoring. Fig. 6a–d show the drop formation from the ejected ink with filament formation until the drops form a sphere.

All printed inks formed spherical drops. For a particle mass fraction between 0 and 5% (see Fig. 6a, b, c) the occurring satellite drops, which formed due to the long filament existence, merged together with the primary drop. For a particle fraction of 10 m%, a stable drop formation could not be observed (see Fig. 6d). Due to thinning, the filament split up into multiple satellite drops that could not merge with the primary drop. Kowalewski [8] postulated that with an increasing viscosity, the flow of the ink from the thinning areas of the filament is reduced and the formation of the neck becomes more pronounced, leading to longer filaments and multiple pinch-offs.

3.5.2. Filament length

The influence of the particle mass fraction on the filament length was determined and is depicted in Fig. 7.

The filament length decreases with an increasing particle fraction until a particle mass fraction of 5% and rises again for a particle mass fraction of 10%. The ink without particles shows the longest filaments. Due to the low frequency, the filament of this ink is longer than with a frequency of 1000 Hz and leads to an instability in the drop formation and thus to a high standard deviation. As already described in SubSection 3.4, the *Z* value at higher frequency resulted in more stable drop formation, but the comparability between the inks was only given at a frequency of 250 Hz. The filament thinning for a particle mass fraction of 10% led to a high scattering of the measurement values and the filament

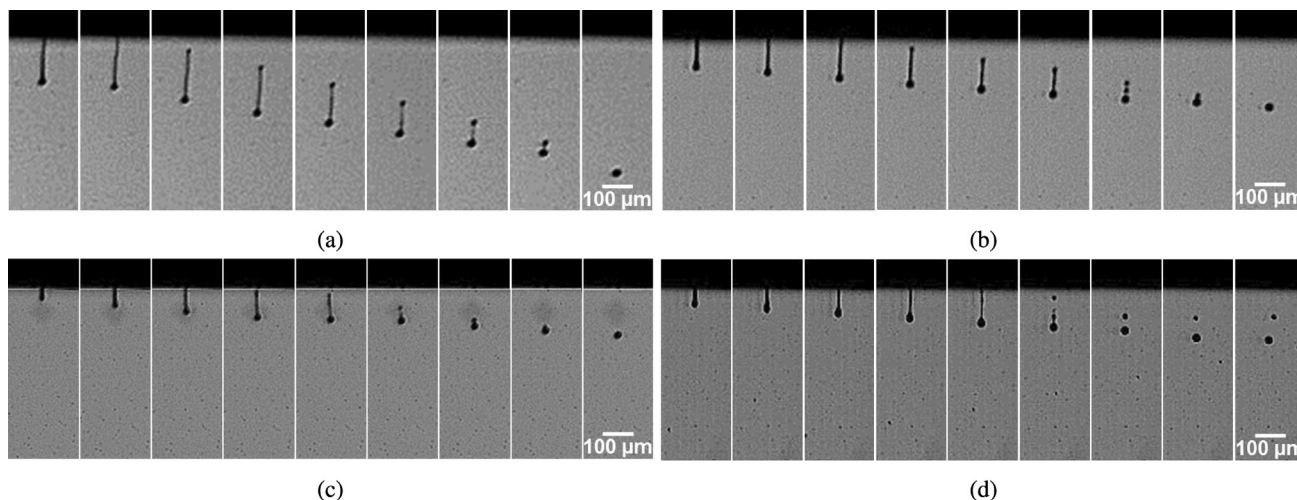


Fig. 6. Drop monitoring images of particle loaded inks with different particle mass fractions; a) no particles, b) 1 m%, c) 5 m%, and d) 10 m%; voltage of 80 V, pulse duration of 7 μs and frequency of 250 Hz; time interval between two adjacent frames of 4 μs

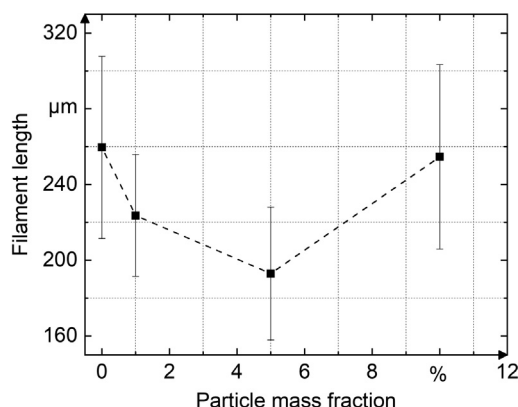


Fig. 7. Filament length of the ejected drops over the particle mass fraction

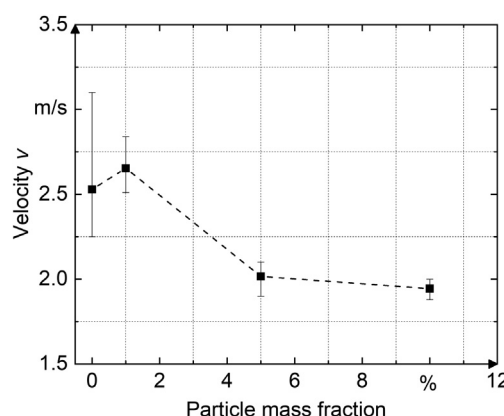


Fig. 8. Drop velocity over the particle mass fraction

lengthened during the drop formation. Due to a higher viscosity, the drop took more time to detach from the nozzle and stretching and thinning of the filament occurred. The decrease of the length at low particle fractions showed that the particles have a positive effect on the filament length. But if the increase in viscosity outweighs the influence of the particles, this effect ceases.

3.5.3. Velocity

The drop velocity is important for the process stability in binder jetting. Marston et al. [10] observed that a high velocity leads to splashing of the drop or the powder and a too low velocity affects the penetration behavior of the droplets into the powder bed. The velocity as a function of the particle fraction is shown in Fig. 8. The ink without particles shows a high scattering of the measurement values because of the long filament, which hinders an accurate measurement. For the particle loaded inks, a correlation between the particle mass fraction and the velocity is observed. The higher the mass fraction of the particles suspended in the ink is, the slower is the velocity of the drops. This observation is consistent with other studies in the literature, such as the study of Tsai et al. [22]. An increase in the particle mass fraction is therefore limited by the resulting velocity. If the drop becomes too slow, it may remain on the powder bed instead of penetrating it.

4. Conclusions

The particle load has a high influence on the drop formation and thus on the process stability in binder jetting. In this study, it was possible to prepare a stable suspended ink and avoid clogging of the print head nozzles. The results of this study can be summarized as follows:

- The particle size distribution is an important measure to determine the formation of agglomerates and to ensure that the set limit for the maximum particle size is not exceeded.
- The dispersant content and the ultrasonic treatment have an influence on the stability of the inks and it was shown that a PVP mass fraction of minimum 20 m% and a duration of the ultrasonic treatment of 160 s are necessary to prepare a stable and sufficiently dispersed particle loaded ink. An increase of the PVP mass fraction and the extension of the duration of the ultrasonic treatment do not improve the dispersion effect.
- The printability of the inks was evaluated by the Z value and validated by the observation of the drop formation conducted by drop monitoring. Inks with a particle load up to 5 m% show a good printability. Exceeding this particle load leads to an increase of the viscosity and a deterioration of the printing behavior. A decrease of the frequency resulted in improved

printability and drop formation, but the ink with a particle load of 10 m% forms undesired satellite drops. The ink with a particle load of 15 m% is too viscous for printing even at a frequency of 250 Hz.

- We demonstrated that the particle load affects the filament length and the velocity of the drops. The particles lead to a reduction of the filament length until increasing the viscosity overrules this effect. The reduction of the velocity can ensure that splashing does not occur during binder jetting, but reducing the speed too much can have a negative effect on the penetration behavior into the powder bed.

In further research, decreasing the viscosity of the base ink can improve the printability of the inks with higher particle loads. Additionally, a base ink with reduced ethylene glycol content will be used. The influence of the particle mass fraction on the penetration behavior in the powder bed is of high interest and will be examined further.

Data availability

The raw data and the processed data required to reproduce these findings can be made available upon request.

Declaration of Competing Interest

The authors declare that they have no known competing financial interests or personal relationships that could have appeared to influence the work reported in this paper.

Acknowledgments

We hereby express our gratitude to the AiF for the funding of this work, within the framework ZIM of the Federal Ministry for Economic Affairs and Energy on the basis of a decision by the German Bundestag. Some of the illustrations and results in this paper were achieved within the scope of the research project "ForAdd-HMTools" (Grant No. 16KN039434).

References

- [1] J.G. Bai, K.D. Creehan, H.A. Kuhn, Inkjet printable nanosilver suspensions for enhanced sintering quality in rapid manufacturing, *Nanotechnology* 18 (2007) 185701, <https://doi.org/10.1088/0957-4484/18/18/185701>.
- [2] B. Derby, Inkjet printing of functional and structural materials: Fluid property requirements, feature stability, and resolution, *Annu. Rev. Mater. Res.* 40 (2010) 395–414, <https://doi.org/10.1146/annurev-matsci-070909-104502>.
- [3] B. Derby, N. Reis, Inkjet printing of highly loaded particulate suspensions, *MRS Bull.* 28 (2003) 815–818, <https://doi.org/10.1557/mrs2003.230>.
- [4] L. Dong, D. Johnson, Surface tension of charge-stabilized colloidal suspensions at the water-air interface, *Langmuir: ACS J. Surfaces Colloids* 19 (2003) 10205–10209, <https://doi.org/10.1021/la035128j>.
- [5] J.E. Fromm, Numerical-calculation of the fluid-dynamics of drop-on-demand jets, *IBM J. Res. Dev.* 28 (1984) 322–333.
- [6] D. Godlinski, S. Morvan, Steel parts with tailored material gradients by 3d-printing using nano-particulate ink, *Mater. Sci. Forum* 492–493 (2005) 679–684, <https://doi.org/10.4028/www.scientific.net/MSF.492-493.679>.
- [7] D. Jang, D. Kim, J. Moon, Influence of fluid physical properties on ink-jet printability, *Langmuir: ACS J. Surfaces Colloids* 25 (2009) 2629–2635, <https://doi.org/10.1021/la900059m>.
- [8] T.A. Kowalewski, On the separation of droplets from a liquid jet, *Fluid Dyn. Res.* 17 (1996) 121–145.
- [9] M. Lehmann, M.F. Zaeh, Process integrated production of wc-co tools with local cobalt gradient fabricated by binder jetting, *Solid Freeform Fabrication Symposium* (2019) 109–121.
- [10] J.O. Marston, S.T. Thoroddsen, W.K. Ng, R. Tan, Experimental study of liquid drop impact onto a powder surface, *Powder Technol.* 203 (2010) 223–236, <https://doi.org/10.1016/j.powtec.2010.05.012>.
- [11] J. Mewis, Flow behaviour of concentrated suspensions: prediction and measurements, *Int. J. Miner. Process.* (1996) 17–27.
- [12] S. Mueller, E.W. Llewellyn, H.M. Mader, The rheology of suspensions of solid particles, *Proc. Roy. Soc. A: Mathe., Phys. Eng. Sci.* 466 (2010) 1201–1228, <https://doi.org/10.1098/rspa.2009.0445>.
- [13] S.M.S. Murshed, S.H. Tan, N.T. Nguyen, Temperature dependence of interfacial properties and viscosity of nanofluids for droplet-based microfluidics, *J. Phys. D: Appl. Phys.* 41 (2008) 85502, <https://doi.org/10.1088/0022-3727/41/8/085502>.
- [14] K.K. Nanda, A. Maisels, F.E. Kruijs, H. Fissan, S. Stappert, Higher surface energy of free nanoparticles, *Phys. Rev. Lett.* 91 (2003) 106102, <https://doi.org/10.1103/PhysRevLett.91.106102>.
- [15] D.A. Polsakiewicz, Herstellung keramischer komposite über den pulverbasierten multi-material 3d-druck Dissertation, Helmut-Schmidt-Universität, Hamburg, 2018.
- [16] D.A. Polsakiewicz, W. Kollenberg, Highly loaded alumina inks for use in a piezoelectric print head, *Materialwiss. Werkstofftech.* 42 (2011) 812–819, <https://doi.org/10.1002/mawe.201100780>.
- [17] Reis, N., Derby, B., 2000. Ink jet deposition of ceramic suspensions: modelling and experiments of droplet formation. *Mat. Res. Soc. Symp. Proc.* 625 (2000).
- [18] Rutgers, Relative viscosity and concentration, *Rheol. Acta* 2 (2) (1962) 305–348.
- [19] F. Schröckert, N. Schifffmann, E.C. Bucharsky, K.G. Schell, M.J. Hoffmann, Tape casted thin films of solid electrolyte lithium-lanthanum-titanate, *Solid State Ionics* 328 (2018) 25–29, <https://doi.org/10.1016/j.ssi.2018.10.028>.
- [20] S. Tanvir, L. Qiao, Surface tension of nanofluid-type fuels containing suspended nanomaterials, *Nanoscale Res. Lett.* 7 (2012) 226, <https://doi.org/10.1186/1556-276X-7-226>.
- [21] J. Traube, Ueber die capillaritätsconstanten organischer stoffe in waeserigen loesungen, *Justus Liebig's Annalen der Chemie* 265 (1891) 27–55, <https://doi.org/10.1002/jlac.18912650103>.
- [22] M.H. Tsai, W.S. Hwang, H.H. Chou, P.H. Hsieh, Effects of pulse voltage on inkjet printing of a silver nanopowder suspension, *Nanotechnology* 19 (2008) 335304, <https://doi.org/10.1088/0957-4484/19/33/335304>.
- [23] Y. Ueki, K. Ueda, M. Shibahara, Thermal conductivity of suspension fluids of fine carbon particles: Influence of sedimentation and aggregation diameter, *Int. J. Heat Mass Transf.* 127 (2018) 138–144, <https://doi.org/10.1016/j.ijheatmasstransfer.2018.06.114>.
- [24] B.R. Utela, D. Storti, R.L. Anderson, M. Ganter, Development process for custom three-dimensional printing (3dp) material systems, *J. Manuf. Sci. Eng.* 132 (2010), <https://doi.org/10.1115/1.4000713>.
- [25] Y. Zhong, H. Fang, Q. Ma, X. Dong, Analysis of droplet stability after ejection from an inkjet nozzle, *J. Fluid Mech.* 845 (2018) 378–391, <https://doi.org/10.1017/jfm.2018.251>.
- [26] H. Zhu, C. Zhang, Y. Tang, J. Wang, B. Ren, Y. Yin, Preparation and thermal conductivity of suspensions of graphite nanoparticles, *Carbon* 45 (2007) 226–228, <https://doi.org/10.1016/j.carbon.2006.07.005>.